



## Clinical and MRI measures to identify non-acute MOG-antibody disease in adults

Rosa Cortese,<sup>1,2</sup> Marco Battaglini,<sup>1</sup> Ferran Prados,<sup>2,3,4</sup> Alessia Bianchi,<sup>2</sup> Lukas Haider,<sup>2</sup> Anu Jacob,<sup>5,6</sup> Jacqueline Palace,<sup>7</sup> Silvia Messina,<sup>7</sup> Friedemann Paul,<sup>8</sup> Jens Wuerfel,<sup>9</sup> Romain Marignier,<sup>10,11</sup> Françoise Durand-Dubief,<sup>10,11</sup> Carolina de Medeiros Rimkus,<sup>12</sup> Dagoberto Callegaro,<sup>13</sup> Douglas Kazutoshi Sato,<sup>14</sup> Massimo Filippi,<sup>15,16,17,18,19</sup> Maria Assunta Rocca,<sup>15,16,19</sup> Laura Cacciaguerra,<sup>15,16,19</sup> Alex Rovira,<sup>20</sup> Jaume Sastre-Garriga,<sup>21</sup> Georgina Arrambide,<sup>21</sup> Yaou Liu,<sup>22</sup> Yunyun Duan,<sup>22</sup> Claudio Gasperini,<sup>23</sup> Carla Tortorella,<sup>23</sup> Serena Ruggieri,<sup>24,25</sup> Maria Pia Amato,<sup>26,27</sup> Monica Ulivelli,<sup>1</sup> Sergiu Groppa,<sup>28</sup> Matthias Grothe,<sup>29</sup> Sara Llufriu,<sup>30</sup> Maria Sepulveda,<sup>30</sup> Carsten Lukas,<sup>31</sup> Barbara Bellenberg,<sup>31</sup> Ruth Schneider,<sup>31,32</sup> Piotr Sowa,<sup>33</sup> Elisabeth G. Celius,<sup>34</sup> Anne-Katrin Proebstel,<sup>35</sup> Özgür Yaldizli,<sup>36</sup> Jannis Müller,<sup>35,36</sup> Bruno Stankoff,<sup>37</sup> Benedetta Bodini,<sup>37</sup> Luca Carmisciano,<sup>38</sup> Maria Pia Sormani,<sup>38</sup> Frederik Barkhof,<sup>2,3,39</sup> Nicola De Stefano,<sup>1,†</sup> and Olga Ciccarelli<sup>2,40,†</sup> for the MAGNIMS Study Group

†These authors contributed equally to this work.

MRI and clinical features of myelin oligodendrocyte glycoprotein (MOG)-antibody disease may overlap with those of other inflammatory demyelinating conditions posing diagnostic challenges, especially in non-acute phases and when serologic testing for MOG antibodies is unavailable or shows uncertain results. We aimed to identify MRI and clinical markers that differentiate non-acute MOG-antibody disease from aquaporin 4 (AQP4)-antibody neuromyelitis optica spectrum disorder and relapsing remitting multiple sclerosis, guiding in the identification of patients with MOG-antibody disease in clinical practice. In this cross-sectional retrospective study, data from 16 MAGNIMS centres were included. Data collection and analyses were conducted from 2019 to 2021. Inclusion criteria were: diagnosis of MOG-antibody disease; AQP4-neuromyelitis optica spectrum disorder and multiple sclerosis; brain and cord MRI at least 6 months from relapse; and Expanded Disability Status Scale (EDSS) score on the day of MRI. Brain white matter T<sub>2</sub> lesions, T<sub>1</sub>-hypointense lesions, cortical and cord lesions were identified. Random forest models were constructed to classify patients as MOG-antibody disease/AQP4-neuromyelitis optica spectrum disorder/multiple sclerosis; a leave one out cross-validation procedure assessed the performance of the models. Based on the best discriminators between diseases, we proposed a guide to target investigations for MOG-antibody disease. One hundred and sixty-two patients with MOG-antibody disease [99 females, mean age: 41 (±14) years, median EDSS: 2 (0–7.5)], 162 with AQP4-neuromyelitis optica spectrum disorder [132 females, mean age: 51 (±14) years, median EDSS: 3.5 (0–8)], 189 with multiple sclerosis (132 females, mean age: 40 (±10) years, median EDSS: 2 (0–8)] and 152 healthy controls (91 females) were studied. In young patients (<34 years), with low disability (EDSS < 3), the absence of Dawson's fingers, temporal lobe lesions and longitudinally extensive lesions in the cervical cord pointed towards a diagnosis of MOG-antibody disease instead of the other two diseases (accuracy: 76%, sensitivity: 81%, specificity: 84%, *P* < 0.001). In these non-acute patients, the number of brain lesions < 6 predicted MOG-antibody disease versus multiple sclerosis (accuracy: 83%, sensitivity: 82%, specificity: 83%, *P* < 0.001). An EDSS < 3 and the absence of longitudinally extensive lesions in the cervical cord predicted MOG-antibody disease versus AQP4-neuromyelitis

optica spectrum disorder (accuracy: 76%, sensitivity: 89%, specificity: 62%,  $P < 0.001$ ). A workflow with sequential tests and supporting features is proposed to guide better identification of patients with MOG-antibody disease. Adult patients with non-acute MOG-antibody disease showed distinctive clinical and MRI features when compared to AQP4-neuromyelitis optica spectrum disorder and multiple sclerosis. A careful inspection of the morphology of brain and cord lesions together with clinical information can guide further analyses towards the diagnosis of MOG-antibody disease in clinical practice.

- 1 Department of Medicine, Surgery and Neuroscience, University of Siena, Siena, Italy
- 2 NMR Research Unit, Queen Square MS Centre, Department of Neuroinflammation, Faculty of Brain Sciences, UCL Queen Square Institute of Neurology, University College London, London, UK
- 3 Center for Medical Imaging Computing, Medical Physics and Biomedical Engineering, UCL, London, UK
- 4 Universitat Oberta de Catalunya, Barcelona, Spain
- 5 NMO Clinical Service at the Walton Centre, Liverpool, UK
- 6 Department of Neurology, Cleveland Clinic, Abu Dhabi, UAE
- 7 Department of Clinical Neurology, John Radcliffe Hospital, Oxford, UK
- 8 Experimental and Clinical Research Center, Max Delbrueck Center for Molecular Medicine and Charité - Universitaetsmedizin Berlin, Berlin, Germany
- 9 Hoffmann LaRoche, Basel, Switzerland
- 10 Department of Biomedical Engineering, University of Basel, Basel, Switzerland
- 11 Service de Neurologie, Sclérose en Plaques, Pathologies de la Myéline et Neuro-inflammation, Hôpital Neurologique Pierre Wertheimer, Hospices Civils de Lyon, Lyon, France
- 12 Departamento de Radiologia e Oncologia, Universidade de São Paulo, Faculdade de Medicina, São Paulo SP, Brazil
- 13 Departamento de Neurologia, Universidade de São Paulo, Faculdade de Medicina, São Paulo SP, Brazil
- 14 Faculdade de Medicina, Pontifícia Universidade Católica do Rio Grande do Sul, Porto Alegre RS, Brazil
- 15 Division of Neuroscience, Neuroimaging Research Unit, IRCCS San Raffaele Scientific Institute, Milan, Italy
- 16 Neurology Unit, IRCCS San Raffaele Scientific Institute, Milan, Italy
- 17 Neurorehabilitation Unit, IRCCS San Raffaele Scientific Institute, Milan, Italy
- 18 Neurophysiology Service, IRCCS San Raffaele Scientific Institute, Milan, Italy
- 19 Vita-Salute San Raffaele University, Milan, Italy
- 20 Section of Neuroradiology, Department of Radiology, Hospital Universitari Vall d'Hebron, Universitat Autònoma de Barcelona, Barcelona, Spain
- 21 Servei de Neurologia-Neuroimmunologia, Centre d'Esclerosi Múltiple de Catalunya (Cemcat), Vall d'Hebron Institut de Recerca, Vall d'Hebron Hospital Universitari, Universitat Autònoma de Barcelona, Barcelona, Spain
- 22 Department of Radiology, Beijing Tiantan Hospital, Capital Medical University, Beijing, China
- 23 Department of Neurosciences, S. Camillo-Forlanini Hospital, Rome, Italy
- 24 Department of Human Neurosciences, Sapienza University of Rome, Rome, Italy
- 25 Neuroimmunology Unit, IRCCS Fondazione Santa Lucia, Rome, Italy
- 26 Department NEUROFARBA, University of Florence, Florence, Italy
- 27 IRCCS Fondazione Don Carlo Gnocchi, Florence, Italy
- 28 Department of Neurology, University Medical Center of the Johannes Gutenberg University Mainz, Mainz, Germany
- 29 Department of Neurology, University Medicine of Greifswald, Greifswald, Germany
- 30 Center of Neuroimmunology, Service of Neurology, Laboratory of Advanced Imaging in Neuroimmunological Diseases, Hospital Clínic of Barcelona, Institut d'Investigacions Biomèdiques August Pi i Sunyer (IDIBAPS), and Universitat de Barcelona, Barcelona, Spain
- 31 St. Josef Hospital, Institute of Neuroradiology, Ruhr University Bochum, Bochum, Germany
- 32 Department of Neurology, St. Josef Hospital, Ruhr University Bochum, Bochum, Germany
- 33 Division of Radiology and Nuclear Medicine, Oslo University Hospital, Oslo, Norway
- 34 Department of Neurology, Oslo University Hospital and Faculty of Medicine, University of Oslo, Oslo, Norway
- 35 Department of Neurology, University Hospital, Kantonsspital, Basel, Switzerland
- 36 Translational Imaging in Neurology (ThINk) Basel, Department of Biomedical Engineering, University Hospital Basel and University of Basel, Basel, Switzerland
- 37 ICM, Pitié Salpêtrière Hospital, Sorbonne University, Paris Brain Institute, Paris, France
- 38 Epidemiology and Biostatistics, University of Genoa, Genoa, Italy
- 39 Radiology and Nuclear Medicine, VU University Medical Centre, Amsterdam, The Netherlands
- 40 National Institute for Health Research (NIHR) University College London Hospitals (UCLH) Biomedical Research Centre, London, UK

Correspondence to: Rosa Cortese, MD, PhD  
Department of Medicine, Surgery and Neuroscience, University of Siena  
Siena, Italy  
E-mail: rosa.cortese@unisi.it

**Keywords:** myelin oligodendrocyte glycoprotein antibody-associated disease; aquaporin 4-antibody positive neuromyelitis optica spectrum disorder; multiple sclerosis; imaging; differential diagnosis

## Introduction

Myelin oligodendrocyte glycoprotein (MOG) antibody (Ab)-associated disease (MOGAD) is a recently recognized demyelinating disease of the CNS, with a highly variable disease course and poorly understood pathogenetic mechanisms.<sup>1</sup> The differentiation between MOGAD and other inflammatory demyelinating diseases, such as relapsing-remitting multiple sclerosis (RRMS) and aquaporin-4-Ab-positive neuromyelitis optica spectrum disorder (AQP4-NMOSD) may be challenging, as they share a number of clinical and radiological features.<sup>2</sup> An accurate differentiation between these diseases is crucial, however, to recommend an effective treatment and predict prognosis.<sup>3,4</sup>

MOGAD can be diagnosed with high specificity by the detection of serum antibodies using anti-MOG antibody cell-based assays (CBA).<sup>5</sup> However, up to a quarter of positive results may be false when the test is performed indiscriminately in a real-life clinical setting (particularly when the titre is low or results are borderline), with MS being the most represented alternative diagnosis.<sup>6</sup> On the other hand, MOG-Ab titres may fluctuate, with some patients turning negative in the non-acute phases of the disease.<sup>7,8</sup> Differences in assay methods may impact on the results of CBA, and discrepancies in low positive or borderline tests may require further investigation.<sup>9</sup> Finally, intrathecal production of MOG-Ab was found in up to 28.9% of seronegative cases, thus suggesting that performing only the blood test might underestimate the real prevalence of MOGAD.<sup>10–13</sup> It is therefore important to identify more stringent measures accompanying MOG-Ab testing to better interpret test results, especially among patients with low antibody titres and atypical phenotypes.

CSF restricted oligoclonal bands can help the identification of MOGAD. In contrast to MS, oligoclonal bands are typically found in a minority of MOGAD patients (about 15%) tested acutely, while they can turn negative on subsequent testing in the non-acute phase.<sup>14</sup> The fluctuation of CSF findings may help to gauge the likelihood of false-positive MS patients being included in MOGAD and to guide treatment strategies. However, a second lumbar puncture is rarely performed in clinical practice.

Distinctive MRI lesional features in MOGAD, AQP4-NMOSD and RRMS have been reported, particularly in acute patients.<sup>7,15</sup> Brain and spinal cord lesions may resolve completely in MOGAD patients, more often than in AQP4-NMOSD and MS, and some acute T<sub>2</sub> lesions can leave small foci of T<sub>2</sub> hyperintensity, thus making the identification of typical signatures more challenging in the chronic phases.<sup>16</sup> Additionally, MOGAD can be clinically heterogeneous, and in the long term, the course of the disease does not generally reflect the severity of the attacks, which can lead to misdiagnosis.<sup>17</sup>

Given the rarity of MOGAD, most of the previous imaging works included a relatively small number of patients or were conducted in a single-centre setting, limiting the generalizability of the results. Moreover, only few and relatively small studies have assessed MOGAD patients in the non-acute phases.<sup>16,18–20</sup>

Against this background, we carried out a study aimed at identifying key features that enable non-acute adult MOGAD to be distinguished from AQP4-NMOSD and RRMS. Our ultimate goal was to provide advice on how to identify MOGAD patients in clinical practice by suggesting sequential tests and supporting features beyond or in addition to serological testing.

## Materials and methods

### Study design and population

This is a multicentre, retrospective cross-sectional study, conducted on previously collected data from 16 international centres [13 Magnetic Resonance Imaging in Multiple Sclerosis (MAGNIMS) collaboration ([www.magnims.eu](http://www.magnims.eu)) centres and three additional centres, respectively, from Europe, Asia and Latin America]. The collection and analysis of the MRI scans was centralized in a single centre (Siena, Italy) from 2019 to 2021.

Inclusion criteria were (i) diagnosis of MOGAD (which was made, in each centre, only when MOGAD was suspected on the basis of patient's history and clinical presentation and was confirmed by MOG antibody positivity according to local laboratory guidelines), AQP4-NMOSD<sup>21</sup> or RRMS<sup>22</sup>; (ii) serum antibodies detected using CBA (either live or fixed); (iii) age at MRI  $\geq$  18 years; (iv) being at least 6 months after an acute event; (v) Expanded Disability Status Scale (EDSS) score at the time of MRI; and (vi) information on type of clinical onset [classified as: isolated optic neuritis (unilateral or bilateral), transverse myelitis, concurrent optic neuritis and transverse myelitis, acute disseminated encephalomyelitis (ADEM), others], age, sex and disease duration (time from disease onset to MRI). Healthy controls (HC) were also recruited. Exclusion criteria were a history of other known medical conditions that could have affected the brain and MRI-related contraindications.

Each participant provided written consent for research within each centre. The final protocol for the analysis of fully anonymized scans, acquired independently at each centre, was approved by the European MAGNIMS collaboration and by the local ethics committees.

### MRI acquisition and processing

Brain and cervical cord images were acquired at 16 sites on 1.5 and 3 T scanners from different manufacturers and with different scanning parameters based on local protocols, following the MAGNIMS guidelines<sup>23</sup> (Supplementary Table 1). All images were visually checked and analysed centrally. Brain white matter lesions were segmented with a semiautomated process using lesion prediction algorithm<sup>24</sup> as implemented in the LST toolbox version for SPM on 3D fluid-attenuated inversion recovery (FLAIR) and proton density/T<sub>2</sub>-weighted MRI sequences. The quality of all the obtained lesions was manually checked and corrected by two experienced

readers (R.C. and M.B.). Lesion volumes were subsequently obtained. Brain MRI scans were examined for Dawson's fingers, juxtacortical lesions in the U-fibre (with a curved/s-shaped morphology), lesions located in the temporal lobes and fluffy infratentorial lesions (FIT), which were found to enable discrimination between MOGAD, AQP4-NMOSD and RRMS.<sup>7</sup> Hypointense lesions on T<sub>1</sub> were automatically identified based on a voxel-by-voxel analysis of the local T<sub>1</sub> ratio value within each lesion mask, adopting a previous definition of hypointense lesion as a region with a signal intensity lower than <1 standard deviation (SD) similar to or reduced compared with the signal intensity of the grey matter of the slice of the lesion and corresponding to a lesion mask drawn on T<sub>2</sub>-weighted MRI. Cortical lesions were assessed on the double inversion recovery (DIR), phase sensitive inversion recovery (PSIR) or magnetization prepared rapid gradient echo (MPRAGE) images, when available, and the presence of cervical cord lesions was recorded, and they were classified as either short lesions or longitudinally extensive cord lesions. We included only cervical cord MRI, as this is the part of the spinal cord most frequently scanned in clinical practice; other segments (i.e. thoracic, lumbar and sacral cord) were available only for a minority of subjects (10% of the whole cohort). The analyses were based on the consensus between two raters (R.C. and L.H.), who had an excellent inter-rater agreement (96% Cohen kappa coefficient).

All readers worked independently and were blinded to clinical data.

## Statistical analyses

The analysis of this study was divided in two parts as below.

### Differences between groups

Means, medians and proportions of demographics, clinical features and MRI measures were calculated for patients and HC. Differences were evaluated using Kruskal–Wallis, ANOVA or  $\chi^2$ , as appropriate.

### Best MRI and clinical discriminators between diseases

The data collection was retrospectively performed using scans already acquired with different MRI protocols and only images of adequate quality were retained. Therefore, not all patients had all sequences and relative measures available. To make efficient use of the available data, we used multiple imputation of missing values for missing data. Imputation was performed using chained equations,<sup>25</sup> where each incomplete variable is imputed by a separate model and implemented through the 'mice' R package. Continuous variables (age, disease duration, EDSS, white matter lesion number and volume, T<sub>1</sub> hypointense lesions and cortical lesion number) were parameterized as numeric data and imputed with the predictive mean matching method, whereas polytomous logistic regression was used for the unordered categorical variables (such as phenotype at onset), and binomial logistic regression for the binary variables (presence/absence of temporal lobe lesions, U-fibre lesions, Dawson's finger type lesions, FIT, cortical lesions, cord lesions). Clinical and available lesion data were used to impute missing lesion data.

To assess the best set of variables for prediction purpose, we ran a random forest selected predictor, with the 3-step procedure,<sup>26</sup> considering first the three diseases together and then one disease versus the other. Eight separate models were constructed using MRI data (i.e. lesion number, volume and morphological characteristics) alone first and then MRI and clinical data (i.e. age, disease

duration, phenotype at onset, EDSS) together. To assess the performance of the selected best predictors in discriminating the diseases, a leave one out internal cross-validation (LOOCV) procedure using the leave one out internal-validation procedure of random forest and binomial logistic regression model was performed using the set of MRI and MRI and clinical together variables. LOOCV is a cross-validation that considers each observation as the validation set and the rest ( $n - 1$ ) as the training set; the process is repeated for all observations such that  $n$  models are estimated and performance averaged. From all models, we obtained the logarithm odds ratio (logOR) of having one disease versus the other, the model average accuracy and kappa coefficient, and the area under (AUC) the receiver operated characteristic (ROC) curve. The analyses were repeated, considering only patients with at least one brain or cervical cord lesion.

Finally, for the selected variables, a Youden index optimization criterion was used to identify the best cut-off (i.e. the value associated with the highest sensibility and sensitivity) that predicted the outcome (e.g. a diagnosis of MOGAD rather than the other two diseases).

Sensitivity analyses were run by repeating all the analyses in a model, including only patients with complete data with no imputation and using a leave one-centre-out procedure rerunning the analysis on data from all but one centre and then validating on the centre not included in train dataset. This was repeated for each centre and reported as average accuracy.

## Data availability

Fully anonymized data are available from each participating centre on request.

## Results

### Study population

Overall, we included 665 subjects in the study: 162 MOGAD, 162 AQP4-NMOSD, 189 RRMS and 152 HC. Demographic and clinical details of subjects are summarized in [Table 1](#). Details about Ab-testing and diagnosis timing are provided in [Supplementary Table 2](#).

### Differences in brain and cervical cord MRI measures between groups

Brain T<sub>2</sub> white matter lesions were detected in 68% of MOGAD, 82% of AQP4-NMOSD, 100% of RRMS patients and 23% of HC. The number of T<sub>2</sub> white matter lesions and corresponding T<sub>1</sub> hypointense lesions on T<sub>1</sub> was lower in the two Ab-mediated diseases than RRMS ( $P < 0.001$ ). Temporal lobe lesions and Dawson's finger-type lesions were detected in a lower percentage of patients in the MOGAD and AQP4-NMOSD cohorts than RRMS (all  $P < 0.001$ ). At least one cortical lesion was seen in 9% of patients with MOGAD, 8% of patients with AQP4-NMOSD and 64% of patients with RRMS. At least one cervical cord lesion was found in a minority of patients with MOGAD (8.6% with short lesions and 1.2% longitudinally extensive lesions), while in a high percentage of patients with AQP4-NMOSD (14.2% with short lesions and 23.5% longitudinally extensive lesions) and those with RRMS (33.9% with short lesions and 1.1% longitudinally extensive lesions) (all  $P < 0.001$ ). None of the HC showed temporal lobe and Dawson's finger-type lesions, cortical and cord lesions; therefore, they were excluded from the discriminant analysis ([Table 2](#)).



Table 1 Clinical features of MOGAD, AQP4-NMOSD, RRMS and HC

| Features  | MOGAD              | AQP4-NMOSD    | RRMS          | HC            | P-value <sup>a</sup> |
|---|--------------------|---------------|---------------|---------------|----------------------|
| n   | 162                | 162           | 189           | 152           |                      |
| Sex, male/female <sup>b</sup>                                     | 63/99              | 30/132        | 57/132        | 61/91         | 0.004                |
| Age at MRI, years, mean (SD)                                      | 40.59 (14.09)      | 50.65 (14.14) | 39.66 (10.44) | 37.38 (11.43) | <0.001               |
| Age at onset, years, mean (SD)                                    | 34.43 (14.33)      | 42.87 (15.69) | 32.27 (8.57)  | NA            | 0.005                |
| Disease duration, years, mean (SD)                                | 5.8 (7.5)          | 8.5 (8.2)     | 7.8 (6.8)     | NA            | <0.001               |
| Time from last attack to MRI, months, <sup>c</sup> median (range) | 14 (3–404)         | 24 (3–263)    | 17 (3–225)    | NA            | 0.01                 |
| EDSS at MRI, median (range)                                       | 2 (0–7.5)          | 3.5 (0–8)     | 2 (0–8)       | NA            | <0.001               |
| Race/ethnicity, n (%) patients                                    |                    |               |               |               | <0.001               |
| Caucasian   | 116 (72)           | 108 (67)      | 144 (76)      | 93 (61)       |                      |
| Asian   | 9 (6)              | 11 (7)        | 7 (4)         | 10 (7)        |                      |
| Afro-Caribbean  | 19 (12)            | 28 (17)       | 11 (6)        | 5 (3)         |                      |
| Mixed   | 3 (2)              | 9 (6)         | 6 (3)         | 3 (2)         |                      |
| Unknown   | 15 (8)             | 6 (3)         | 21 (11)       | 41 (27)       |                      |
| Patients on treatment, n (%)                                      | 78 (48)            | 144 (88)      | 189 (100)     | NA            | <0.001               |
| Type of treatment <sup>d</sup> , n (%) patients                   |                    |               |               |               | <0.001               |
| MS disease modifying agents                                       | 2 (2)              | 0             | 181 (96)      | NA            |                      |
| Classical immunosuppressants                                      | 73 (94)            | 134 (93)      | 7 (3)         | NA            |                      |
| Other immunosuppressants  | 3 (4)              | 10 (7)        | 1 (1)         | NA            |                      |
| Phenotype at onset, n (%) patients                                |                    |               |               |               | <0.001               |
| Unilateral optic neuritis   | 44 (27)            | 44 (27)       | 38 (20)       | NA            |                      |
| Bilateral optic neuritis  | 36 (22)            | 11 (7)        | 3 (2)         | NA            |                      |
| Transverse myelitis   | 38 (24)            | 55 (34)       | 38 (20)       | NA            |                      |
| Optic neuritis + transverse myelitis                              | 17 (11)            | 16 (10)       | 1 (1)         | NA            |                      |
| ADEM  | 9 (6)              | 0             | 1 (1)         | NA            |                      |
| Others  | 8 (5) <sup>e</sup> | 16 (10)       | 77 (41)       | NA            |                      |
| Disease course, n (%) patients                                    |                    |               |               |               | <0.001               |
| Monophasic  | 48 (32)            | 23 (16)       | 0             | NA            |                      |
| Relapsing   | 100 (68)           | 118 (84)      | 189 (100)     | NA            |                      |
| Number of patients (%) with CSF oligoclonal bands                 |                    |               |               |               | <0.001               |
| Absence   | 102 (84%)          | 86 (75%)      | 10 (10%)      | NA            |                      |
| Presence  | 19 (16%)           | 22 (25%)      | 93 (90%)      | NA            |                      |

<sup>a</sup>Using Kruskal–Wallis, ANOVA or  $\chi^2$ , as appropriate, depending on the nature of the variable.

<sup>b</sup>Refers to biological factors. This information was self-reported by participants.

<sup>c</sup>A minority of patients presented with a relapse within 3 and 6 months prior to study entry, respectively, 40/162 (25%) of MOGAD, 27/162 (17%) of AQP4-NMOSD and 50/189 (26%) of RRMS patients.

<sup>d</sup>MS disease modifying agents included medications approved for MS: interferon, glatiramer acetate, teriflunomide, dimethylfumarate, cladribine, fingolimod, natalizumab, alemtuzumab, ocrelizumab; classical immunosuppressants included: azathioprine, mycophenolate mofetil, rituximab; other immunosuppressants included: cyclophosphamide, methotrexate, mitoxantrone.

<sup>e</sup>Seven patients with brainstem involvement, one patient with unilateral tumefactive hemispheric lesion.

## MRI and clinical discriminators between diseases

After imputation, 456 (88.9%) patients were included in the analysis. [Supplementary Table 3](#) reports the proportion of missing values for each clinical and MRI measure, which were homogeneously distributed among the three diseases.

### MOGAD versus AQP4-NMOSD versus RRMS

When considering the three diseases together, the MRI measures that predicted MOGAD instead of the other two diseases were the absence of Dawson's fingers, temporal lobe lesions and longitudinally extensive lesions in the cord [average accuracy: 68%, sensitivity: 82%, specificity: 66%, AUC: 0.75, 95% confidence interval (CI): 72–80,  $P < 0.001$ ]. Adding disability level and age at MRI increased the sensitivity of the model (average accuracy: 76%, sensitivity: 81%, specificity: 84%, AUC: 0.85, 95% CI: 0.82–0.88,  $P < 0.001$ ) ([Fig. 1](#) and [Table 3](#)).

When considering only patients with at least one brain or cervical cord lesion, the model selected the same best set of MRI measures, which reached the highest accuracy in predicting MOGAD

rather than AQP4-NMOSD and RRMS (average accuracy: 70%, sensitivity: 68%, specificity: 72%, AUC: 0.75, 95% CI: 0.71–0.78,  $P < 0.001$ ). Adding disability increased the sensitivity of the model (average accuracy: 79%, sensitivity: 67%, specificity: 83%, AUC: 0.84, 95% CI: 0.80–0.87,  $P < 0.001$ ).

The best cut-off value was 3 for predicting the diagnosis of MOGAD with respect to EDSS; 34 years with respect to age.

### MOGAD versus RRMS

The lower number of brain lesions was the best MRI measure that distinguished non-acute MOGAD from RRMS (average accuracy: 76%, sensitivity: 80%, specificity: 73%, AUC: 0.87, 95% CI: 0.83–0.91,  $P < 0.001$ ). This means that for each unit decrease of lesion there is a 9% reduced risk of having MOGAD instead of RRMS.

When considering only patients with at least one lesion, the combination of lower number of brain lesions and the absence of Dawson's fingers reached the highest accuracy in predicting MOGAD instead of RRMS (average accuracy: 79%, sensitivity: 78%, specificity: 80%, AUC: 0.85, 95% CI: 0.80–0.90,  $P < 0.001$ ). The best cut-

Table 2 MRI features of MOGAD, AQP4-NMOSD, RRMS and HC

| Features  | MOGAD              | AQP4-NMOSD          | RRMS                | HC               | P-value <sup>a</sup> |
|---|--------------------|---------------------|---------------------|------------------|----------------------|
| Brain lesion volume, mm <sup>3</sup>  | 82.60              | 416.76              | 4231.10             | 0.002            | <0.001               |
| Median (range)  | (0.00–851.25)      | (0.00–2739.75)      | (1392.08–11736.75)  | (0.00–1.80)      |                      |
| Total number of brain WML; mean (SD)  | 1047; 6.80 (12.11) | 1604; 10.69 (14.13) | 4925; 26.62 (21.16) | 144; 2.21 (5.27) | <0.001               |
| Total Number of T <sub>1</sub> hypointense lesions; mean (SD)                         | 647; 7.7 (9.7)     | 976; 8.4 (10.6)     | 3749; 13.8 (16.4)   | 92; 1.4 (4.7)    | <0.001               |
| Presence of temporal lobe lesion, number of patients (%) <sup>b</sup>                 |                    |                     |                     |                  | <0.001               |
| Absence   | 138 (85)           | 143 (88.3)          | 74 (39.2)           | 152 (100)        |                      |
| Presence  | 14 (8.6)           | 9 (5.6)             | 111 (58.7)          | 0                |                      |
| Presence of U-fibre lesion, number of patients (%) <sup>b</sup>                       |                    |                     |                     |                  | <0.001               |
| Absence   | 147 (90.7)         | 148 (91.4)          | 161 (85.2)          | 152 (100)        |                      |
| Presence  | 5 (3.1)            | 4 (2.5)             | 24 (12.7)           | 0                |                      |
| Presence of Dawson's finger lesion, number of patients (%) <sup>b</sup>               |                    |                     |                     |                  | <0.001               |
| Absence   | 135 (83.3)         | 145 (89.5)          | 50 (26.5)           | 152 (100)        |                      |
| Presence  | 17 (10.5)          | 7 (4.3)             | 135 (71.4)          | 0                |                      |
| Presence of FIT lesion, number of patients (%) <sup>b</sup>                           |                    |                     |                     |                  | <0.001               |
| Absence   | 149 (92.0)         | 151 (93.2)          | 183 (96.8)          | 152 (100)        |                      |
| Presence  | 3 (1.9)            | 1 (0.6)             | 2 (1.1)             | 0                |                      |
| Presence of cortical lesions, number of patients (%) <sup>b</sup>                     |                    |                     |                     |                  | <0.001               |
| Absence   | 88 (91)            | 87 (92)             | 40 (36)             | 152 (100)        |                      |
| Presence  | 9 (9)              | 8 (8)               | 70 (64)             | 0                |                      |
| Total number of cortical lesions  | 19                 | 8                   | 172                 | 0                | <0.001               |
|   | 6 intracortical    | 0 intracortical     | 51 intracortical    |                  |                      |
|   | 13 leukocortical   | 8 leukocortical     | 121 leukocortical   |                  |                      |
| Median (range) <sup>b</sup>   | 1 (1–9)            | 1 (1–1)             | 2 (1–14)            |                  |                      |
| Presence of short cord lesion, number of patients (%) <sup>b</sup>                    |                    |                     |                     |                  | <0.001               |
| Absence   | 93 (57.4)          | 77 (47.5)           | 51 (27.0)           | 152 (100)        |                      |
| Presence  | 14 (8.6)           | 23 (14.2)           | 64 (33.9)           | 0                |                      |
| Presence of longitudinally extensive cord lesion, number of patients (%) <sup>b</sup> |                    |                     |                     |                  | <0.001               |
| Absence   | 105 (64.8)         | 62 (38.3)           | 113 (59.8)          | 152 (100)        |                      |
| Presence  | 2 (1.2)            | 38 (23.5)           | 2 (1.1)             | 0                |                      |

WML = white matter lesions.

<sup>a</sup>Using Kruskal-Wallis, ANOVA or  $\chi^2$ , as appropriate, depending on the nature of the variable.

<sup>b</sup>Assessed on available sequences.

off value was 6 with respect to the number of lesions that predicted the diagnosis of MOGAD.

If the phenotype at onset was either bilateral optic neuritis, concurrent optic neuritis and transverse myelitis or ADEM, the sensitivity of the model to distinguish the two diseases increased either when using the whole sample (average accuracy: 83%, sensitivity: 82%, specificity: 83%, AUC: 0.89, 95% CI: 0.85–0.93,  $P < 0.001$ ) or when selecting patients with at least one lesion (average accuracy: 81%, sensitivity: 58%, specificity: 91%, AUC: 0.86, 95% CI: 0.81–0.91,  $P < 0.001$ ).

### MOGAD versus AQP4-NMOSD

The absence of longitudinally extensive lesions in the cord was the best MRI measure for distinguishing MOGAD from AQP4-NMOSD, either when considering all patients (average accuracy: 67%, sensitivity: 97%, specificity: 37%, AUC: 0.67, 95% CI: 0.63–0.71,  $P < 0.001$ ) or when only patients with at least one lesion were selected (average accuracy: 65%, sensitivity: 94%, specificity: 47%, AUC: 0.32, 95% CI: 0.27–0.38,  $P < 0.001$ ).

When considering MRI and clinical measures together, the sensitivity of the model to predict MOGAD increased if low EDSS was considered (average accuracy: 76%, sensitivity: 89%, specificity: 62%, AUC: 0.83, 95% CI: 0.78–0.88,  $P < 0.001$ ), reaching the highest accuracy when only patients with at least one lesion were considered (average accuracy: 84%, sensitivity: 84%, specificity: 68%, AUC: 0.80, 95% CI: 0.74–0.86,  $P < 0.001$ ).

The best cut-off value was three with respect to the EDSS for predicting the diagnosis of MOGAD.

### AQP4-NMOSD versus RRMS

The absence of Dawson's fingers and temporal lobe lesions were the best discriminators between AQP4-NMOSD and RRMS, either when using MRI measures only or MRI and clinical measures together (average accuracy: 87%, sensitivity: 89%, specificity: 62%, AUC: 0.89, 95% CI: 0.86–0.93,  $P < 0.001$ ). This was confirmed when considering only patients with at least one lesion, which was when the highest rate of accuracy was reached (average accuracy: 88%, sensitivity: 89%, specificity: 85%, AUC: 0.89, 95% CI: 0.85–0.92,  $P < 0.001$ ). [Supplementary Table 4](#) summarizes the performances of the best MRI and clinical measures in discriminating between the diseases. [Supplementary Tables 5 and 6](#) report details on the analyses performed when considering only patients with at least one lesion.

All sensitivity analyses confirmed these findings; the same sets of best discriminators between diseases were selected when using only complete baseline data with no imputation, with a high average accuracy between centre validation performance ([Supplementary Tables 7 and 8](#)).

Finally, in [Fig. 2](#), we propose a workflow that can be applied to non-acute adult patients with suspected CNS inflammatory disease to help in the identification of MOGAD in clinical practice. [Figure 3](#) shows representative MRIs of MOGAD patients with different clinical and MRI characteristics.

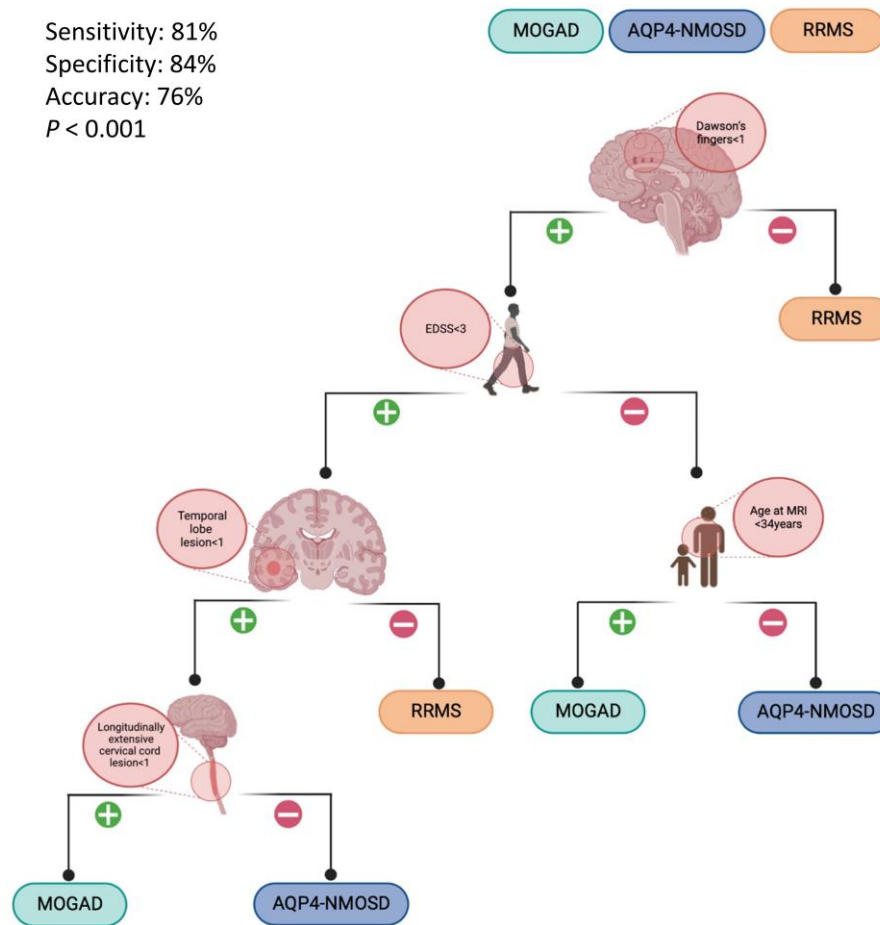


**Figure 1** Visual representation of the best set of discriminators between MOGAD, AQP4-NMOSD and RRMS. Example of a random tree from a leave one out internal-validation procedure of a random forest model, showing the MRI and clinical measures that predicted MOGAD instead of AQP4-NMOSD and RRMS. The order of measures in the tree represents the most (Dawson's fingers) to the less (longitudinally extensive lesions in the cervical cord) accurate discriminator. Image was created using BioRender (<https://biorender.com/>).

## Discussion

In this large, multicentre study, we identified MRI and clinical features to differentiate non-acute MOGAD from RRMS and AQP4-NMOSD and proposed a workflow that may serve as a guide towards a better discrimination of MOGAD.

Results of the study showed that brain lesion number and morphology are important in distinguishing patients with non-acute MOGAD from those with RRMS, while clinical features and cervical cord involvement can differentiate the two Ab-mediated diseases. Absence of Dawson's fingers and temporal lobe lesions might lead to the questioning of a RRMS diagnosis, especially in patients with low disability outside an acute event. Previous studies showed that, in MOGAD, lesions may disappear after the acute phase and often resolve completely over 6 months, potentially reflecting a greater propensity for remyelination.<sup>16,27</sup> Therefore, it is not surprising that in our cohort lesion characteristics considered to be specific for acute MOGAD (i.e. FIT lesions)<sup>28</sup> were found only in a minority of patients and did not contribute to the discriminant analysis. This is in agreement with the previous report of reduced visibility of infratentorial lesions in MOGAD patients when evaluated in the remission phase.<sup>19</sup> We found white matter lesions in 68% of MOGAD patients, which was higher than expected, as disease phenotypes at onset were optic neuritis and/or transverse myelitis for the majority of patients.<sup>20</sup> Imaging characteristics are

age-dependent in MOGAD, with the highest frequency of brain involvement in children, ranging from poorly demarcated and widespread lesions in childhood to small non-specific cerebral lesions in older children and adults.<sup>29</sup> This discordance may be due to the inclusion in our study of only adult patients, who may have had incidental white matter hyperintensities. In support of this, white matter lesions were found in 23% of HC, suggesting that discriminating demyelinating white matter lesions from those of presumably vascular origin may be challenging in adults during the non-acute phase. Indeed, future plans are to expand our cohorts with a paediatric subgroup with the same demyelinating conditions to assess the effect of age.

Data presented here showed that the differentiation between non-attack MOGAD and AQP4-NMOSD scans might be more challenging but can be achieved when clinical information is available. In patients with low disability levels, the absence of cervical longitudinally extensive cord lesions on a spinal cord MRI supports the diagnosis of MOGAD. By contrast, in our cohort, the presence of longitudinally extensive lesions in the cord did not favour MOGAD over MS in patients. This can be explained as follows: (i) longitudinally extensive lesions occurs in MOGAD more often in the caudal spinal cord than in the cervical cord, which was the segment evaluated in this study; and (ii) cord lesions tend to disappear and a complete resolution of these lesions on conventional MRI in the non-acute phase has been reported.<sup>16</sup>

Table 3 Results from the LOOCV of random forest model using the best sets of discriminators and the imputed set of data

|                                      | Variable importance <sup>a</sup> |            |      | Mean decrease in impurity <sup>b</sup> | Mean decrease in accuracy <sup>c</sup> | Accuracy (LOOCV) <sup>d</sup> | Kappa (LOOCV) <sup>d</sup> | AUC (95% CI) <sup>e</sup> |
|--------------------------------------|----------------------------------|------------|------|--|--|-------------------------------|----------------------------|---------------------------|
|                                      | MOGAD                            | AQP4-NMOSD | RRMS |  |  |                               |                            |                           |
| MRI                                  |                                  |            |      |  |  |                               |                            |                           |
| Dawson's fingers lesion              | 77.4                             | 5.3        | 58.6 | 72.9                                   | 88.4                                   | 0.68                          | 0.52                       | 0.75 (0.72–0.78)          |
| Temporal lobe lesion                 | 71.7                             | 12.4       | 31   | 16.3                                   | 72                                     |                               |                            |                           |
| Longitudinally extensive cord lesion | 42.6                             | 76.1       | 26   | 23.4                                   | 73                                     |                               |                            |                           |
| Clinical and MRI                     |                                  |            |      |  |  |                               |                            |                           |
| Dawson's fingers lesion              | 48.1                             | 34.9       | 38.5 | 55.6                                   | 65.2                                   | 0.76                          | 0.64                       | 0.85 (0.82–0.88)          |
| Temporal lobe lesion                 | 39.9                             | 20.2       | 15.3 | 30.9                                   | 42.7                                   |                               |                            |                           |
| Longitudinally extensive cord lesion | 36.4                             | 30.0       | 12.9 | 19.5                                   | 41.4                                   |                               |                            |                           |
| Age at MRI                           | −0.4                             | 15.2       | 10.9 | 43.0                                   | 14.8                                   |                               |                            |                           |
| EDSS                                 | 23.1                             | 33.8       | 9.4  | 40.4                                   | 36.8                                   |                               |                            |                           |

<sup>a</sup>Variable importance represents the difference between the prediction errors (on the out-of-bag portion of the data) and the prediction error after performing random predictor permutations. Showing the class-specific (MOGAD, AQP4-NMOSD, RRMS) error we attempt to give extra information about which predictors are important for which class.

<sup>b</sup>Mean decrease in impurity uses the Gini index, which is a measure of impure classification ranging from 0 (totally clear) to 1 (totally random). When removing a variable from a model (such as in random variable permutation procedures) the corresponding Gini drop of a variable is a measure of the usefulness of such variable to improve the classification performance (the higher the better).

<sup>c</sup>Mean decrease in accuracy, also known as permutation importance, is a measure of the usefulness of a variable within a random permutation procedure using the proportion of correctly classified cases (i.e. accuracy) as internal metrics instead of impurity. It is more computationally expensive than mean decrease in impurity but may offer more reliable estimates when predictors are of mixed data type (categorical and continuous).

<sup>d</sup>Leave one out validation accuracy and kappa represent the internal model stability and gives us insight on the generalizability of our conclusions in the attempt to mitigate the natural overfit tendency of our model-based predictions. Accuracy is the proportion of correctly classified subjects among all the cross-validation cycle. For example, an accuracy of 0.7 means that 7 times out of 10 the model should correctly classify a subject not previously seen during model training. This can overestimate performances if once class is overrepresented. Kappa is a similar metric but account for the marginal probabilities of the classes and therefore adjust the accuracy for the simplicity of correctly classify the most prevalent class only by chance.

<sup>e</sup>AUC represents the area under the ROC curve. It is used here as a simple metric for summarizing the performance of different classification models (based on a different set of predictors i.e. MRI only or MRI and clinic variables).

Our data emphasises the importance of cord lesion length in differentiating the three diseases, which may be even higher when considering patients in the acute phases, as about 85% of cervical acute lesions span more than three vertebral segments in AQP4-NMOSD, while they are typically rare in MOGAD and MS.<sup>15</sup> While longitudinally extensive hazy T<sub>2</sub> hyperintensities may be detected outside attacks in chronic MS, chronic lesions can be short in AQP4-NMOSD and MOGAD, therefore making the differentiation between the three diseases more challenging.<sup>15,30</sup> Further studies looking at different cord segments, including thoracolumbar/conus regions that are preferentially involved in MOGAD, and different disease phases are needed to quantify the overall extent of cord damage accurately in the three diseases. Nonetheless, our results suggest that cord MRI findings have significant value in differentiating patients with CNS demyelinating diseases from controls and may be useful in identifying those with non-specific brain white matter lesions. This is supported by the absence of cord lesions in the HC versus the disease groups when compared with the frequency of brain lesions in healthy subjects.

By contrast, in patients with high disability levels, MOG-Ab testing should be limited to patients who are young at the time of MRI. Previous studies have reported that, compared with NMOSD, accumulated disability in MOGAD as calculated on the EDSS over time is less severe, but in the majority of these studies, AQP4-NMOSD patients were older at the time of observation.<sup>17</sup> In cases of patients with CNS inflammation negative to both Ab and with no features typical of MS, it is important to consider mimics of CNS demyelination and monitor the patient over time.

A recent study showed that serial MRIs have limited utility in MOGAD, as silent new lesions are rare outside a clinical attack, in

contrast to MS, where new brain lesions can be found independently of relapses.<sup>31</sup> Importantly, our findings may help to select those patients in whom surveillance MRI is necessary. In MOGAD, where lesions often resolve over time, rather than enlarge, and new lesions rarely develop, a single follow-up remission brain and cervical cord MRI may have added value in establishing the diagnosis and provide valuable information to overcome false-positive results or delayed MOG-Ab testing.

As we used brain and cord images acquired with different MRI protocols from different centres, we performed an internal cross-validation using LOOCV, which improves the generalizability of the predictions. We found high concordance between centres in the selection of best discriminators between diseases, suggesting that one can reliably use brain and cervical cord MRI along with clinical information to separate the three diseases, independently of scanner characteristics, and results could be generalized to other centres. Cross-validation methods are useful when the dataset is not very large: an advantage of using cross-validation is that there is no waste of data. When we have an external validation set, the data used for validation are wasted and never used for training, but in cross-validation, we use the validation set for training due to the resampling approach. However, limitations of LOOCV include the highly variable validation error for a given model and that it is a computationally intensive method. Further, external validation would be warranted to consolidate our results. However, to account for the possible confounding by the imputation of missing values, we also repeated the analysis on a subset of subjects with complete, non-imputed data and confirmed the predictors of diseases, suggesting the robustness of our results.



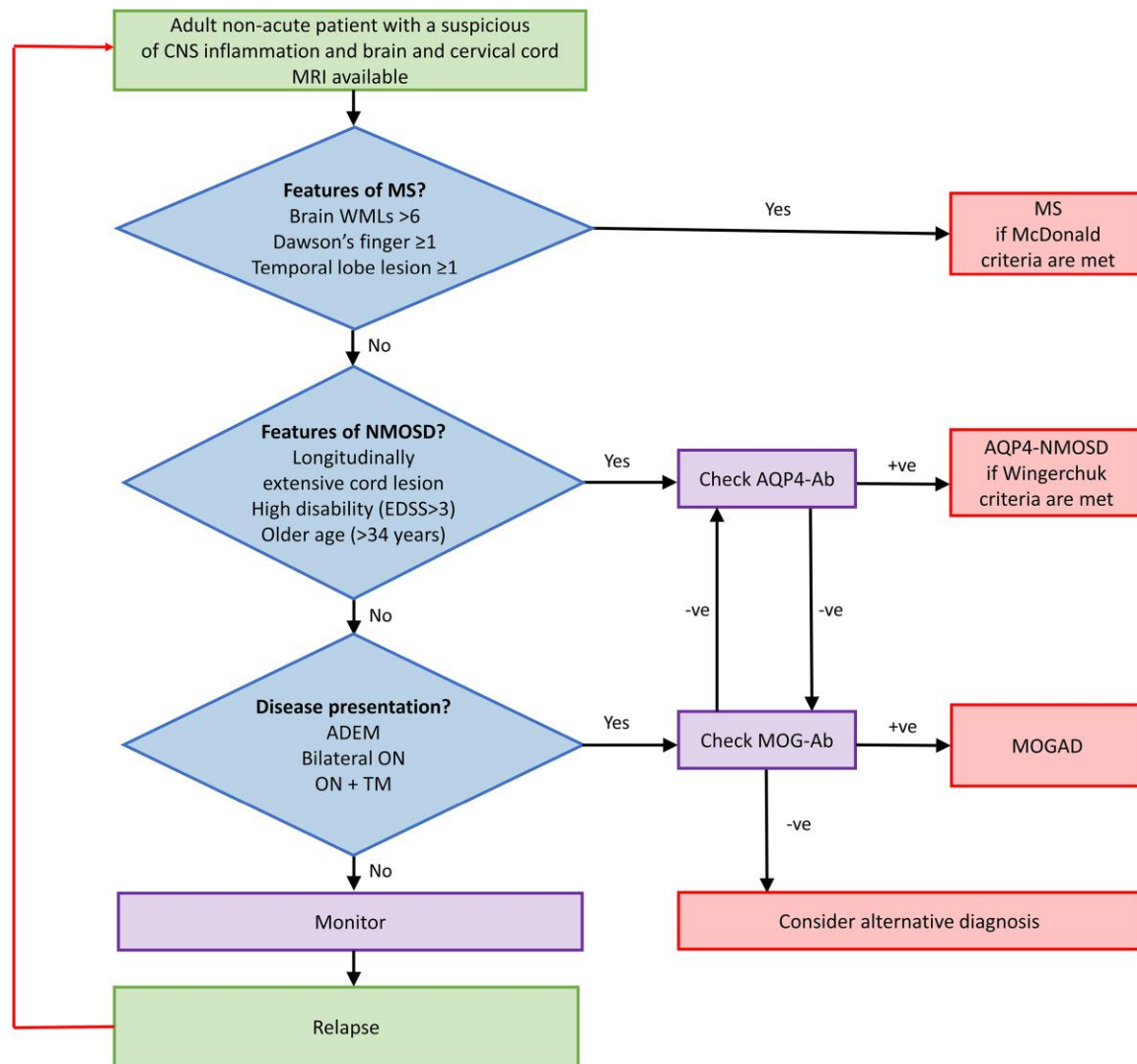


**Figure 2** Workflow that can be applied to non-acute adult patients with suspected CNS inflammatory disease to help in the identification of MOGAD. The first recommended approach is to assess disease history and MRI findings. If MRI features resemble MS [i.e. high number of white matter lesions (>6), presence of Dawson's fingers and temporal lesions], the McDonald criteria should be applied,<sup>18</sup> which may allow a diagnosis of MS. Alternatively, in patients who have clinical and MRI characteristics suggestive of NMOSD, AQP4-Ab testing may permit a diagnosis of AQP4-NMOSD if Wingerchuk criteria are met,<sup>17</sup> particularly in patients having a cervical longitudinally extensive cord lesion, high disability (EDSS > 3) at the time of MRI, and older than 34 years. In AQP4-Ab negative patients, if disease presentation is considered to be typical or suggestive of MOGAD [i.e. ADEM, bilateral optic neuritis, concomitant optic neuritis and transverse myelitis), then MOG-Ab should be checked. In MOG-Ab positive cases, this helps to reach the diagnosis of MOGAD. In patients with ADEM, bilateral optic neuritis, concomitant optic neuritis and transverse myelitis, concurrently without longitudinally extensive lesions in the cervical cord or high disability who resulted MOG-Ab negative, AQP4-Ab should be checked. Consideration of alternative diagnoses, and then monitoring are recommended in the remaining Ab-negative patients. ON = optic neuritis; TM = transverse myelitis; WML = white matter lesion; +ve = positive; -ve = negative.

In addition to the limitations related to validation, there are limitations related to the dataset and the study design. First, although this is to our knowledge the largest study combining MRI and clinical features to discriminate MOGAD from AQP4-NMOSD and RRMS, only patients with a confirmed diagnosis were included in the study. Therefore, the results are not easily generalizable to patients at the time of the first presentation of the disease and patients with seronegative NMOSD. Second, the time interval between MRI and the previous relapse and the scan frequency differed between patient groups, with the potential bias of having more scans in patients with more severe or atypical disease. Third, the retrospective design did not allow us to assess the role of CSF findings (i.e. presence/absence of oligoclonal bands), as this

information was only available for a subgroup of patients, and optic nerve lesions, which are common in MOGAD, in discriminating the diseases, as dedicated sequences were not acquired by the majority of centres. Finally, we could not consider lesions that disappear over time, which might occur in MOGAD, due to the cross-sectional design of this study. A future prospective, longitudinal study will test whether the absence of oligoclonal bands (or if present at all, their persistence after the non-acute phase), the involvement of the optic nerve and lesion evolution over time can increase the accuracy of our approach to identify MOGAD.

In line with previous studies, cortical lesions were seen in a minority of patients with MOGAD and AQP4-NMOSD.<sup>19,20</sup> Reversible cortical involvement in MOGAD has been described in patients

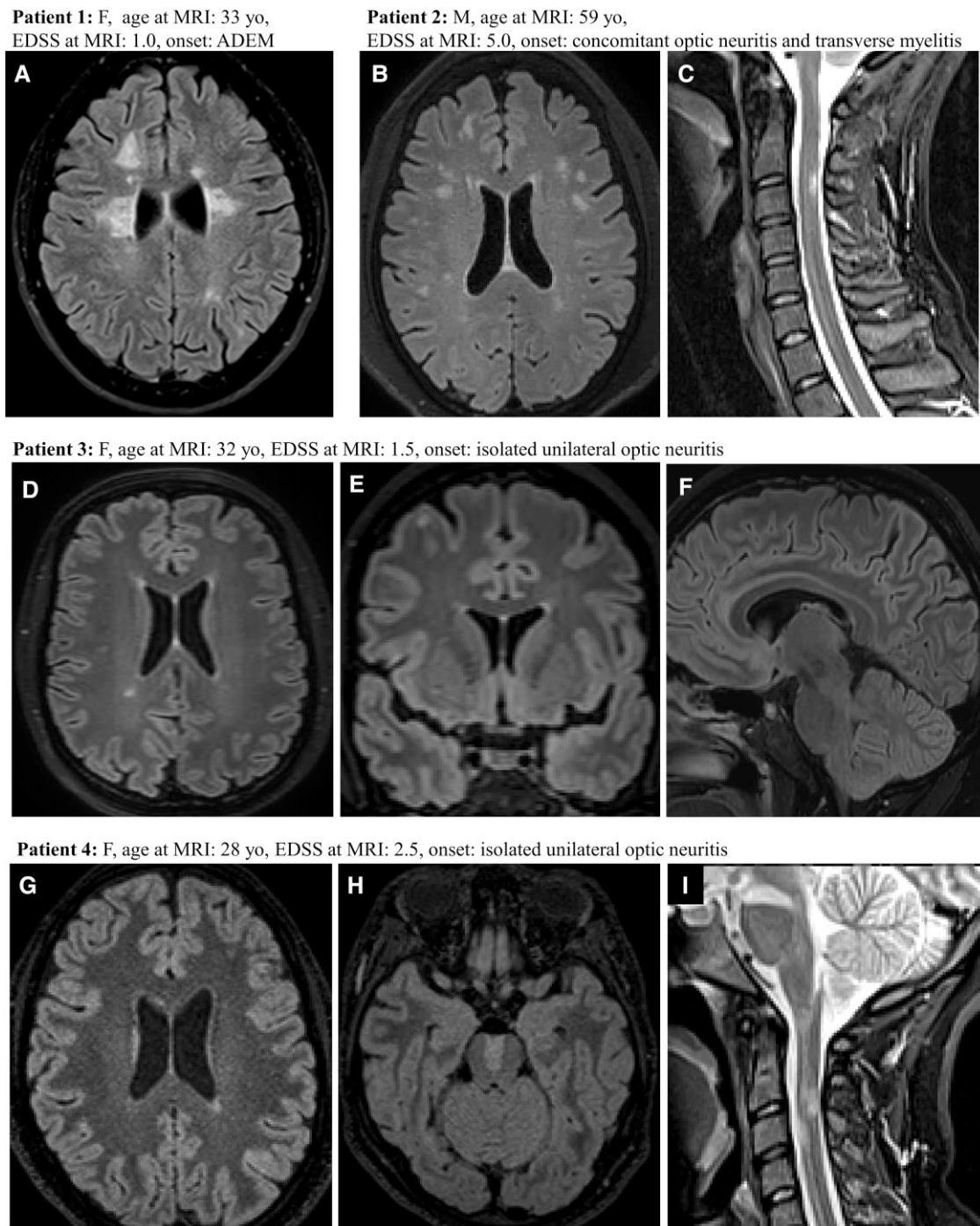


**Figure 3** Representative examples of MRI findings in non-acute MOGAD patients and different clinical and MRI characteristics. Patients with disease presentation typical of MOGAD: (A) Patient 1 showing poorly margined brain lesions; (B and C) Patient 2 with more than six brain white matter lesions and one short cervical cord lesion. Patients with isolated unilateral optic neuritis at onset: (D–F) Patient 3 showing less than six brain white matter lesions, with no involvement of temporal lobes and no Dawson’s fingers; (G–I) Patient 4: one periventricular lesion, brainstem involvement and two short cord lesions.

presenting with encephalopathy and/or seizures, while cortex is typically spared in NMOSD.<sup>32,33</sup> When detected, cortical lesions in AQP4-NMOSD may have a vascular rather than demyelinating origin, as patients may be more hypercoagulable (e.g. antiphospholipid Ab commonly coexist in AQP4-Ab positive patients) and are typically older; thus, small asymptomatic cortical infarcts may occur.<sup>34</sup> Similarly, the number of T<sub>1</sub> hypointense lesions in the two Ab-mediated diseases was lower than in RRMS, as expected due

to the different brain involvement in the three disorders. Surprisingly, both measures were not included as best discriminating measures by the model. This is in contrast with recent findings suggesting a role of cortical lesions in differentiating between NMOSD and RRMS.<sup>35</sup> A possible explanation for this may be the lower number of patients as well as the reduced availability of sequences to perform the cortical lesion analysis when compared with T<sub>2</sub> lesions assessment. Similarly, as T<sub>2</sub> and T<sub>1</sub> lesions are

correlated, only T<sub>2</sub> lesions were selected by the statistical model, which was built to detect only the best set of variables for prediction using stringent criteria.

Currently, there are no evidence-based guidelines for the non-acute treatment and management of MOGAD patients.<sup>1</sup> From a clinical perspective, we hypothesize that our guide will allow targeted investigation and timely changes in treatment strategies, as the decision to initiate chronic immunosuppression in MOGAD is more controversial than in AQP4-NMOSD, and MS treatments were shown to be ineffective in the two Ab-mediated diseases.<sup>36,37</sup>

Future studies are needed to confirm whether our suggested approach can be used to differentiate the three diseases at an early stage (i.e. after the first attack) or in other challenging clinical scenarios (i.e. including seronegative NMOSD and controls with focal white matter lesions presumably of vascular origin).

In conclusion, in this large and multicentre study, we found that brain and cord lesion characteristics as detected by conventional MRI, together with routine demographic and clinical information, may facilitate an accurate differentiation between MOGAD, AQP4-NMOSD and RRMS in the non-acute phases. On this basis, we have provided a guide for clinicians that could complement Ab-testing when results are controversial or when CBA testing is not readily available.

## Acknowledgements

The authors thank Dr Yael Hacohen for her thoughtful comments on the study, Dr Lise Magnollay for the recruitment of patients from the London cohort, Dr Claudia Chien, Patrick Schindler, Dr Eva Maria-Birgit Dorsch and Dr Rebekka Rust for the information of patients from the Berlin cohort.

## Funding

The present research was conducted thanks to the 2019ECTRIMS-MAGNIMS fellowship (awarded to R.C.).

## Competing interests

R.C. was awarded a MAGNIMS-ECTRIMS fellowship in 2019. F.P. received a Guarantors of Brain fellowship 2017–2020 and is supported by National Institute for Health Research (NIHR), Biomedical Research Centre initiative at University College London Hospitals (UCLH). J.P. received support for scientific meetings and honorariums for advisory work from Merck Serono, Biogen Idec, Novartis, Teva, Chugai Pharma, Bayer Schering, Alexion, Roche, Genzyme, MedImmune, EuroImmune, MedDay, Abide ARGEX, UCB and Viela Bio and grants from Merck Serono, Novartis, Biogen Idec, Teva, Abide, MedImmune, Bayer Schering, Genzyme, Chugai and Alexion. She has received grants from the Multiple Sclerosis Society UK, Guthy Jackson Foundation, National Institute of Health Research, Oxford Health Services Research Committee, Medical Research Council, GMSI (Grant for MS Innovation), John Fell, Myaware and AMPLO for research studies. F.P. serves on scientific advisory boards for Novartis, Viela Bio, Alexion and has received speaker honoraria from Bayer, Teva, Merck, Viela, Alexion, Roche and Novartis. J.W. is an employee of Hoffmann LaRoche, Basel, Switzerland and has consulted Actelion/Johnson&Johnson, Biogen, Genzyme-Sanofi, Idorsia, Novartis, Roche and Teva. He has received funding from EU (HORIZON2020); none of this is related

to the present study. C.D.R. has received speaker honoraria from Roche Pharma. D.K.S. received research support from CNPq/Brazil (425331/2016–4 and 308636/2019–8), FAPERGS/Brazil (17/2551-0001391-3 and 21/2551-0000077-5), Teva, Merck, Biogen for investigator-initiated studies, and speaker honoraria from Biogen, Merck and Roche, and participated in advisory boards for Biogen, Roche, and Merck. M.F. is Editor-in-Chief of the *Journal of Neurology* and Associate Editor of *Human Brain Mapping*; received compensation for consulting services and/or speaking activities from Almirall, Alexion, Bayer, Biogen Idec, Celgene, Eli Lilly, Genzyme, Merck-Serono, Novartis, Roche, Sanofi, Takeda, and Teva Pharmaceutical Industries; and receives research support from Biogen Idec, Merck-Serono, Novartis, Roche, Teva Pharmaceutical Industries, Italian Ministry of Health, Fondazione Italiana Sclerosi Multipla, and ARiSLA (Fondazione Italiana di Ricerca per la SLA). M.A.R. received speakers' honoraria from Bayer, Biogen Idec, Bristol Myers Squibb, Celgene, Genzyme, Merck Serono, Novartis, Roche and Teva, and receives research support from the MS Society of Canada and Fondazione Italiana Sclerosi Multipla. L.C. received speaker and consultant honoraria from ACCMED, Roche, BMS Celgene, and Sanofi. A.R. serves on scientific advisory boards for Novartis, Sanofi-Genzyme, Synthetic MR, Roche, Biogen, TensormMedical and OLEA Medical, and has received speaker honoraria from Bayer, Sanofi-Genzyme, Merck-Serono, Teva Pharmaceutical Industries Ltd., Novartis, Roche and Biogen. J.S-G. received personal fees from Biopass, Biogen, Celgene, Merck and Orchid Pharma. He is member of the Editorial Committee of *Multiple Sclerosis Journal* and Director of the Scientific Committee of *Revista de Neurologia*. G.A. has received compensation for consulting services or participation in advisory boards from Sanofi, Merck, and Roche; research support from Novartis; travel expenses for scientific meetings from Novartis, Roche, Stendhal and ECTRIMS; and speaking honouraria from Sanofi, Merck and Roche. G.A. is the editor for Europe of the *Multiple Sclerosis Journal—Experimental, Translational and Clinical*, and is a member of the executive committee of the International Women in Multiple Sclerosis (iWiMS) network. C.G. received fees as invited speaker or travel expenses for attending meeting from Biogen, Merck-Serono, Teva, Mylan, Sanofi, Novartis, Genzyme. C.T. received honoraria for speaking and travel grants from Biogen, Sanofi-Aventis, Merck Serono, Bayer-Schering, Teva, Genzyme, Almirall and Novartis. M.P.A. has served on Scientific Advisory Boards for Biogen, Novartis, Roche, Merck, Sanofi Genzyme and Teva; speaker honoraria from Biogen, Merck, Sanofi Genzyme, Roche, Novartis and Teva; and research grants for her Institution from Biogen, Merck, Sanofi Genzyme, Novartis and Roche. M.G. has received compensation for serving on Scientific Advisory Boards for Novartis, Roche and Sanofi Genzyme; he received speaker honoraria and travel support from Merck, Novartis, Roche, Sanofi Genzyme and Teva; he received research support from Novartis. S.L. received compensation for consulting services and speaker honoraria from Biogen Idec, Novartis, TEVA, Genzyme, Sanofi and Merck. M.S. received speaking honoraria from Roche and UCB Pharma, and travel reimbursement from Biogen, Sanofi and Zambon for national and international meetings. C.L. received a research grant by the German Federal Ministry for Education and Research, BMBF, German Competence Network Multiple Sclerosis (KKNMS, grant no.01GI1601I) and has received consulting and speaker's honoraria from Biogen Idec, Bayer Schering, Daiichi Sanykyo, Merck Serono, Novartis, Sanofi, Genzyme and TEVA. R.S. has received



consulting and speakers' honoraria from Biogen Idec GmbH and Roche Pharma AG and has received research scientific grant support from Novartis Pharma. E.G.C. has received honoraria for lecturing and advice from Biogen, Merck and Roche, grants and honoraria from Novartis and Sanofi. A.K.P. has participated as speaker in meetings sponsored by and received consulting fees and/or grant support from Biogen and Roche. Ö.Y. received grants from ECTRIMS/MAGNIMS, University of Basel, Pro Patient Stiftung University Hospital Basel, Free Academy Basel, Swiss Multiple Sclerosis Society and advisory board/lecture and consultancy fees from Roche, Sanofi Genzyme, Allmirall, Biogen and Novartis. B.S. has received grants and personal fees for lectures from Roche, Sanofi-Genzyme, and Merck-Serono, personal fees for lectures from Novartis, Biogen and Teva. B.B. has received traveling and speaker's honoraria from Novartis, Genzyme, Roche and Merck Serono, and she received research support from Biogen. M.P.S. received consulting fees from Biogen, Merck, Roche, Novartis, Sanofi, Immunic, GeNeuro. F.B. is supported by the NIHR Biomedical Research Centre initiative at UCLH, and he serves on the editorial boards of *Brain*, *European Radiology*, *Journal of Neurology*, *Neurosurgery & Psychiatry*, *Neurology*, *Multiple Sclerosis*, and *Neuroradiology*, and serves as consultant for Bayer Schering Pharma, Sanofi-Aventis, Biogen-Idec, TEVA Pharmaceuticals, Genzyme, Merck-Serono, Novartis, Roche, Synthon, Jansen Research, and Lundbeck. N.D. has received honoraria from Biogen-Idec, Bristol Myers Squibb, Celgene, Genzyme, Immunic, Merck Serono, Novartis, Roche and Teva for consulting services, speaking, and travel support. He serves on advisory boards for Merck, Novartis, Biogen-Idec, Roche, and Genzyme, Immunic and he has received research grant support from the Italian MS Society. O.C. received research funding from NIHR Biomedical Research Centre initiative at UCLH, UK and National MS Societies, Rosetrees trust; she is an Associate Editor for *Neurology*. The other authors report no competing interests. All coauthors had full access to all the data in the study and take responsibility for the integrity of the data and the accuracy of the data analysis.

## Supplementary material

Supplementary material is available at *Brain* online.

## Appendix 1

Full details are provided in the [Supplementary material](#).

The authors are members of the MAGNIMS network (Magnetic Resonance Imaging in MS; <https://www.magnims.eu/>), which is a group of European clinicians and scientists with an interest in undertaking collaborative studies using MRI methods in multiple sclerosis, independent of any other organization and is run by a steering committee whose members are: F. Barkhof, N. de Stefano, J. Sastre-Garriga, O. Ciccarelli, C. Enzinger, M. Filippi, C. Gasperini, L. Kappos, J. Palace, H. Vrenken, Á. Rovira, M.A. Rocca and T. Yousry.

## References

- Marignier R, Hachohen Y, Cobo-Calvo A, et al. Myelin oligodendrocyte glycoprotein antibody-associated disease. *Lancet Neurol*. 2021;20:762-772.
- Flanagan EP. Neuromyelitis optica spectrum disorder and other non-multiple sclerosis central nervous system inflammatory diseases. *Contin Lifelong Learn Neurol*. 2019;25:815-844.
- Tajfirouz DA, Bhatti MT, Chen JJ. Clinical characteristics and treatment of MOG-IgG-associated optic neuritis. *Curr Neurol Neurosci Rep*. 2019;19:100.
- Hachohen Y, Banwell B. Treatment approaches for MOG-ab-associated demyelination in children. *Curr Treat Options Neurol*. 2019;21:2.
- Jarius S, Ruprecht K, Kleiter I, et al. MOG-IgG in NMO and related disorders: A multicenter study of 50 patients. Part 1: Frequency, syndrome specificity, influence of disease activity, long-term course, association with AQP4-IgG, and origin. *J Neuroinflammation*. 2016;13:279.
- Sechi E, Buciu M, Pittock SJ, et al. Positive predictive value of myelin oligodendrocyte glycoprotein autoantibody testing. *JAMA Neurol*. 2021;78:741-746.
- Juryńczyk M, Tackley G, Kong Y. Brain lesion distribution criteria distinguish MS from AQP4-antibody NMOSD and MOG-antibody disease. *J Neurol Neurosurg Psychiatry*. 2017;88:132-136.
- Marchionatti A, Woodhall M, Waters PJ, Sato DK. Detection of MOG-IgG by cell-based assay: Moving from discovery to clinical practice. *Neurol Sci*. 2021;42:73-80.
- Reindl M, Schanda K, Woodhall M, et al. International multicenter examination of MOG antibody assays. *Neurol Neuroimmunol Neuroinflamm*. 2020;7:e674.
- Akaishi T, Takahashi T, Misu T, et al. Difference in the source of anti-AQP4-IgG and anti-MOG-IgG antibodies in CSF in patients with neuromyelitis optica spectrum disorder. *Neurology*. 2021;97:e1-e12.
- Jarius S, Lechner C, Wendel EM, et al. Cerebrospinal fluid findings in patients with myelin oligodendrocyte glycoprotein (MOG) antibodies. Part 2: Results from 108 lumbar punctures in 80 pediatric patients. *J Neuroinflammation*. 2020;17:262.
- Mariotto S, Gajofatto A, Batzu L, et al. Relevance of antibodies to myelin oligodendrocyte glycoprotein in CSF of seronegative cases. *Neurology*. 2019;93:E1867-E1872.
- Kwon YN, Kim B, Kim JS, et al. Myelin oligodendrocyte glycoprotein-immunoglobulin G in the CSF. *Neurol Neuroimmunol Neuroinflamm*. 2022;9:e1095.
- Jarius S, Ruprecht K, Kleiter I, et al. MOG-IgG in NMO and related disorders: a multicenter study of 50 patients. Part 2: Epidemiology, clinical presentation, radiological and laboratory features, treatment responses, and long-term outcome. *J Neuroinflammation*. 2016;13:280.
- Ciccarelli O, Cohen JA, Reingold SC, et al. Spinal cord involvement in multiple sclerosis and neuromyelitis optica spectrum disorders. *Lancet Neurol*. 2019;18:185-197.
- Sechi E, Krecke KN, Messina SA, et al. Comparison of MRI lesion evolution in different central nervous system demyelinating disorders. *Neurology*. 2021;97:e1097-e1109.
- Lopez-Chiriboga S, Sechi E, Buciu M, et al. Long-term outcomes in patients with myelin oligodendrocyte glycoprotein immunoglobulin G-associated disorder. *JAMA Neurol*. 2020;77:1575-1577.
- Mariano R, Messina S, Kumar K, Kuker W, Leite MI, Palace J. Comparison of clinical outcomes of transverse myelitis among adults with myelin oligodendrocyte glycoprotein antibody vs aquaporin-4 antibody disease. *JAMA Netw open*. 2019;2:e1912732.
- Messina S, Mariano R, Roca-Fernandez A, et al. Contrasting the brain imaging features of MOG-antibody disease, with AQP4-antibody NMOSD and multiple sclerosis. *Mult Scler*. 2022;28:217-227.



20. Cortese R, Prados Carrasco F, Tur C, et al. Differentiating multiple sclerosis from AQP4-neuromyelitis optica spectrum disorder and MOG-antibody disease with imaging. *Neurology*. 2023;100:e308–e323.
21. Wingerchuk DM, Banwell B, Bennett JL, et al. International consensus diagnostic criteria for neuromyelitis optica spectrum disorders. *Neurology*. 2015;85:177–189.
22. Thompson AJ, Banwell BL, Barkhof F, et al. Diagnosis of multiple sclerosis: 2017 revisions of the McDonald criteria. *Lancet Neurol*. 2018;17:162–173.
23. Wattjes MP, Ciccarelli O, Reich DS, et al. 2021 MAGNIMS–CMSC–NAIMS consensus recommendations on the use of MRI in patients with multiple sclerosis. *Lancet Neurol*. 2021; 20:653–670.
24. LST—Lesion segmentation for SPM | Paul Schmidt—freelance statistician. Accessed July 19, 2021. <https://www.applied-statistics.de/lst.html>
25. Burgess S, White IR, Resche-Rigon M, Wood AM. Combining multiple imputation and meta-analysis with individual participant data. *Stat Med*. 2013;32:4499–4514.
26. Genuer R, Poggi J-M, Tuleau-Malot C. *Variable selection using random forests*. Accessed June 22, 2021. <http://www.r-project.org/>
27. Uzawa A, Mori M, Kuwabara S. Different patterns of brainstem and cerebellar MRI abnormalities in demyelinating disorders with MOG and aquaporin-4 antibodies. *J Neurol Neurosurg Psychiatry*. 2021;92:348.
28. Jurynczyk M, Geraldine R, Probert F, et al. Distinct brain imaging characteristics of autoantibody-mediated CNS conditions and multiple sclerosis. *Brain*. 2017;140:617–627.
29. Baumann M, Grams A, Djurdjevic T, et al. MRI Of the first event in pediatric acquired demyelinating syndromes with antibodies to myelin oligodendrocyte glycoprotein. *J Neurol*. 2018;265: 845–855.
30. Ciron J, Cobo-Calvo A, Audoin B, et al. Frequency and characteristics of short versus longitudinally extensive myelitis in adults with MOG antibodies: a retrospective multicentric study. *Mult Scler*. 2020;26:936–944.
31. Syc-Mazurek S B, Chen JJ, Morris P, et al. Frequency of new or enlarging lesions on MRI outside of clinical attacks in patients with MOG-antibody-associated disease. *Neurology*. Published online September 29, 2022:10.1212/WNL.0000000000201263.
32. Salama S, Khan M, Levy M, Izbudak I. Radiological characteristics of myelin oligodendrocyte glycoprotein antibody disease. *Mult Scler Relat Disord*. 2019;29:15–22.
33. Calabrese M, Oh MS, Favaretto A, et al. No MRI evidence of cortical lesions in neuromyelitis optica. *Neurology*. 2012;79:1671–1676.
34. Asgari N. Epidemiological, clinical and immunological aspects of neuromyelitis optica (NMO). *Dan Med J*. 2013;60:B4730.
35. Cacciaguerra L, Meani A, Mesaros S, et al. Brain and cord imaging features in neuromyelitis optica spectrum disorders. *Ann Neurol*. 2019;85:371–384.
36. Cobo-Calvo A, Sepúlveda M, Rollot F, et al. Evaluation of treatment response in adults with relapsing MOG-ab-associated disease. *J Neuroinflammation*. 2019;16:1–12.
37. Jacob A, Hutchinson M, Elson L, et al. Does natalizumab therapy worsen neuromyelitis optica? *Neurology*. 2012;79: 1065–1066.